University of Baghdad
College of Engineering
JE
JOURNAL OF ENGINEERING

Journal of Engineering

journal homepage: www.jcoeng.edu.iq

Volume 31 Number 3 March 2025

Linear Active Disturbance Rejection Control (ADRC) for Two Wheel Self-Balancing Robot

Noor Abdul Ameer *, Ibraheem Kasim Ibraheem

Department of Electrical Engineering, College of Engineering, University of Baghdad, Baghdad, Iraq

ABSTRACT

The application of two-wheeled self-balancing robots to real-world tasks critically depends on their ability to actively reject disturbances. The objective is to design two active disturbance rejection controllers (ADRCs) for body angle and displacement, respectively, for a two-wheeled self-balancing robot system, which is difficult to control due to strong coupling, nonlinearity, and parameter uncertainty. Based on the system dynamics, an ADRC control framework is designed to estimate and compensate for modeling errors and disturbances online. Numerical simulations are used to demonstrate the effectiveness of ADRC in different controller combinations, using Simulink MATLAB 2022a and tuning parameters by genetic algorithm (GA) to ensure good temporal performance and assist in the design parameter selection process. Studies on a real two-wheeled self-balancing vehicle show that the constructed ADRC scheme allows the vehicle to operate more than 90% more stably and effectively than the assumed control strategy, which can effectively realize the self-balancing and steering process with the performance of fast adjustment speed, high accuracy, and strong robustness as well when compared with the PID (proportional-integral-derivative) controller under the same parameter setting.

Keywords: Two Wheel Self-Balancing Robot (TWSBR), Active Disturbance Rejection Control (ADRC), Proportional-Integral-Derivative (PID) control, Genetic Algorithm (GA).

1. INTRODUCTION

A very unstable wheeled dynamic system with substantial coupling, parameter uncertainty, and nonlinear properties is the two-wheeled self-balancing robot. As a result, it requests a higher level of the controller design **(Ye et al., 2013).** The primary emphasis of research on two-wheeled self-balancing robot controllers is how to select an appropriate control algorithm to produce consistent and dependable control effects of the robot body over an extended period of time. Presently, popular self-balancing algorithms include pole

*Corresponding author
Peer review under the responsibility of University of Baghdad.
https://doi.org/10.31026/j.eng.2025.03.10

Article received: 13/08/2024
Article revised: 22/01/2025
Article accepted: 28/01/2025
Article published: 01/03/2025

placement, LQR, and PID algorithms. The two-wheeled self-balancing robot is very nonlinear; therefore, linearization will result in an imprecise model and suboptimal control consequences. Furthermore, the classic control algorithms' anti-interference capabilities and dynamic reactions are insufficient. Fuzzy control is the primary method of intelligent control; it can manage nonlinear unknown systems without mathematical system modeling, increasing the system's dynamic response and anti-jamming capabilities; however, the fuzzy control algorithm's control accuracy is dependent on the establishment of the fuzzy rule base; as control degree accuracy improves, the number of fuzzy rules grows exponentially. Furthermore, the expert's experience plays a major role in the system's control impact **(Paulescu et al., 2021)**. A control technique that maximizes PID control's features without relying on the plant model is called active disturbance rejection control, or ADRC. It has evolved into a model for the engineering application of contemporary control theory and can handle control issues with high coupling between the various variables by straightforward static decoupling. It has numerous successful engineering applications both domestically and internationally **(Han, 2002; Ibraheem and Ibraheem, 2016)**. In this research, ADRC is used to control a two-wheeled self-balancing robot and produces some very good displacement and angle control results.

Active Disturbance Rejection Control (ADRC) is a well-recognized and established control technique in the field of control. It simplifies the description of the system by grouping all endogenous disturbances, which depend on internal variables such as states, outputs, control inputs, unmolded parametritis, and nonlinearities, and exogenous disturbances, which are caused by external factors like the environment or interactions with other systems **(Sira-Ramírez et al., 2017)**. Since the ADRC views the entire disturbance as an extended state, which is estimated accurately and in real-time by an Extended State Observer (ESO), and subsequently canceled by a feedback control action, its primary characteristic is its estimation/cancellation nature **(Han,2009)**. Because of this characteristic, the ADRC approach is easy to use, elegant, and effective in a wide range of systems, including electric servomechanisms and machines **(Linares-Flores et al.,2015; Linares-Flores et al., 2012; Sira-Ramírez et al., 2014)**, CD/CD power converters **(Sira-Ramírez et al.,2016; Hernández-Méndez et al., 2017)**, renewable energy combined with cooperative control **(Hernández-Méndez et al.,2017)**, and so on.

Active disruption researchers formally presented rejection control, an enhanced PID-based control technique, **(Han, 2009)**. It is composed of three components: the extended state observer (ESO) the tracking differentiator (TD) and the nonlinear state error feedback (NLSEF). The foundational concepts of ADRC are error estimation and compensation. The majority of unknown variables and unmolded plant components can be thought of as the overall disturbance, which ESO can estimate. After that, the control variables are created to make up for the mistakes **(Han, 2009).** As a result, understanding the intricate mathematics of the plant is not required. All that is required of us is the model's order and high-frequency gain. Furthermore, ADRC inherits the benefits of conventional PID control: the removal of variation in accordance with variation. ADRC was first proposed more than 20 years ago, and other specialists have since expanded on it. Among them, **(Gao, 2003)** addressed the nonlinear connection and put out the LADRC idea, which facilitates the selection of control parameters and encourages the continued use of ADRC **(Zheng and Gao, 2016)**. Traditional ADRC tuning techniques are widely available **(Liu et al.,2011; Kang, 2019; Qi et al.,2013).** While LADRC tuning techniques are also widely available **(Tan and Fu, 2017; Li et al., 2015)**.

Underwater robots **(Wang et al.,2019)**, microgrid inverters **(Mtolo et al., 2021)**, linear induction motors **(Alonge et al., 2017)**, and other sectors are among the many applications for ADRC that are currently in use. We are considering applying ADRC control technology to the TWSBV platform in order to enhance its dynamic performance, given its benefits. Because TDs vary so much, control legislation, ESOs, and a variety of ADRC arrangements. Nevertheless, the current successes **(Curiel-Olivares et al., 2021; Abdul-Adheem et al., 2020)**, that combine ADRC with self-balancing vehicles emphasize numerical modeling over physical implementation. Furthermore, it is not obvious to notice the control effects of different structures because there is no comparative simulation of the various ADRC controller architectures.

Through previous experiments and methods used on this system, we find that the proposed method is better in terms of performance, response speed, achieving balance in shorter periods than before, reducing energy consumption, strong durability, and maintaining the required balance in the event of any sudden disturbance.

This article's contributions: Initially, utilized two ADRC controllers focusing on managing the body angle and displacement of TWSBR. Additionally, a genetic algorithm (GA) technique was implemented to enhance performance metrics while also ensuring reduced power wastage. Comparative simulations were carried out between the ADRC designs and their traditional PID counterparts, remarkably confirming that our models provide superior disturbance reduction as well as smoother controller operation. Lastly, various conditions were employed when appraising system improvements in terms of response times, handling disturbances control-wise, and overall robustness.

2. TWSBR MATHEMATICAL MODEL

A two-wheeled self-balancing robot can be thought of as an inverted pendulum installed atop a vehicle, which makes the analysis of its dynamic model more difficult. Newton's equations of motion serve as the foundation for the balanced robot model: Typically, a two-wheeled self-balancing robot is made up of one kind of battery, electronics, controllers, and two wheels fastened to a body frame. The three primary components of system modelling are as follows:

- Linear DC motor model.
- Wheels model.
- Chassis model.

The way a two-wheeled robot that can balance on its own moves straight depends on four things. These are how far it goes in a straight line, how fast it moves, the direction it faces, and how quickly it turns. Obtained the following mathematical model, per reference **(Ye et al., 2013)**:

$$(I_p + M_p l^2)\ddot{\theta}_p - \frac{2K_m K_e}{R r_w}\dot{x} + \frac{2k_m}{R}V_a + M_p g l \sin\theta_p = -M_p l\ \ddot{x}\cos\theta_p \quad (1)$$

The above equation can be rewritten as follows:

$$\ddot{\theta}_p = \frac{1}{(I_p + M_p l^2)}\left(\frac{2k_m k_e}{R r_w}\dot{x} - \frac{2k_m}{R}V_a - M_p g l \sin\theta_p - M_p l\ \ddot{x}\cos\theta_p\right) \quad (2)$$

The above equation can be rewritten as follows:

$$\frac{2k_m}{Rr_w}V_a = (2M_w + \frac{2I_w}{{r_w}^2} + M_p)\ddot{x} + \frac{2k_m k_e}{R{r_w}^2}\dot{x} + M_p l\ \ddot{\theta}_p \cos\theta_p - M_p l\ \dot{\theta}^2 \sin\theta_p \quad (3)$$

$$\ddot{x} = \frac{1}{\left(2M_w + \frac{2I_w}{{r_w}^2} + M_p\right)}\left(-\frac{2k_m k_e}{R{r_w}^2}\dot{x} + \frac{2k_m}{Rr_w}V_a - M_p l\ \ddot{\theta}_p \cos\theta_p + M_p l\ \dot{\theta}^2 \sin\theta_p\right) \quad (4)$$

2.1. Final State Space TWSBR

Four factors determine a two-wheeled self-balancing robot's position and condition as it walks in a straight line: the robot's body's angular velocity, vector and angular velocity, and straight-line displacement. These variables are the robot body's angular velocity ($\dot{\theta p}$), angle (θ_p), straight-line displacement (x_p), and velocity ($\dot{x}_p$). The state space TWSBR that follows is obtained in accordance with **(Ye et al., 2013)**:

$$\begin{bmatrix}\dot{x}_1\\ \dot{x}_2\\ \dot{x}_3\\ \dot{x}_4\end{bmatrix} = \begin{bmatrix} x_2 \\ \frac{\alpha_1+\alpha_2\cos x_1}{1-\lambda_1 cos^2 x_1}x_4 + \frac{\alpha_3 \sin x_1}{1-\lambda_1 cos^2 x_1} + \frac{\alpha_4 sinx_1 \cos x_1}{1-\lambda_1 cos^2 x_1}{x^2}_2 - \frac{\alpha_5+\alpha_6\cos x_1}{1-\lambda_1 cos^2 x_1}U \\ x_4 \\ \frac{\beta_1+\beta_2\cos x_1}{1-\lambda_1 cos^2 x_1}x_4 + \frac{\beta_3 \sin x_1 cosx_1}{1-\lambda_1 cos^2 x_1} + \frac{\beta_4 sinx_1}{1-\lambda_1 cos^2 x_1}{x^2}_2 + \frac{\beta_5+\beta_6\cos x_1}{1-\lambda_1 cos^2 x_1}U \end{bmatrix} \quad (5)$$

Where
$x_1 = \theta_p$, $x_2 = \dot{\theta p}$, $x_3 = x_p$ and $x_4 = \dot{x}_p$

The variables:

$$\lambda_1 = \frac{{M^2}_p\ l^2}{(J_p + M_p l^2)(2M_w + \frac{2J_w}{r_w r^2} + M_p)}\ , \beta_1 = \frac{-2k_m\ k_e}{R{r_w}^2(2M_w + \frac{2J_w}{{r_w}^2} + M_p)}$$

$$\beta_2 = \frac{-2k_m k_e M_p\ l}{Rr_w(J_p + M_p l^2)(2M_w + \frac{2J_w}{{r_w}^2} + M_p)}\ , \beta_3 = \frac{l^2 {M^2}_p\ g}{(J_p + M_p l^2)(2M_w + \frac{2J_w}{{r_w}^2} + M_p)}$$

$$\beta_4 = \frac{M_p\ l}{(2M_w + \frac{2J_w}{{r_w}^2} + M_p)}\ , \beta_5 = \frac{2k_m}{Rr_w(2M_w + \frac{2J_w}{{r_w}^2} + M_p)}\ , \beta_6 = \frac{2k_m M_p l}{(J_p + M_p l^2)(2M_w + \frac{2J_w}{{r_w}^2} + M_p)}$$

$$\alpha_1 = \frac{2k_m k_e}{Rr_w(J_p + M_p l^2)}\ ,\ \alpha_2 = \frac{2k_m k_e M_p\ l}{(J_p + M_p l^2)(2M_w + \frac{2J_w}{{r_w}^2} + M_p)}\ , \alpha_3 = \frac{-M_p g l}{(J_p + M_p l^2)}$$

$$\alpha_4 = \frac{-2{M^2}_p\ l^2}{(J_p + M_p l^2)(2M_w + \frac{2J_w}{{r_w}^2} + M_p)}\ ,\ \alpha_5 = \frac{2k_m}{R(J_p + M_p l^2)}\ ,\ \alpha_6 = \frac{2k_m M_p\ l}{Rr_w(J_p + M_p l^2)(2M_w + \frac{2J_w}{{r_w}^2} + M_p)}$$

3. PROBLEM STATEMENT

The challenge for the controller of this type of system is to maintain TWSBR balance while tracking the intended course on level ground and rejecting disturbances because of the system's high levels of nonlinearity, instability, and parameter uncertainty. The solution is an Active Disturbance Rejection Control (ADRC) structure that consists of a linear Extended

State Observer (LESO) that estimates the total disturbance as well as the system's states, a tracking differentiator (TD), and a PD controller.

4. ACTIVE DISTURBANCE REJECTION CONTROL (ADRC) DESIGN

Generally speaking, ADRC consists of a state and total disturbance observer (e.g., LESO), a signal profile generator (e.g., TD), and a nonlinear controller (e.g., SEF). The features of each of these parts are mentioned below. **Fig.1** depicts the general LADRC's organization. This paper will construct two second-order LADRC units (one for the attitude (x) and two for the altitude (z) subsystems of the 2-DoF TWSBR system. For the TWSBR subsystems, the LESO of the LADRC unit equals two and estimates the states up to the relative degree (ρ) of each subsystem **(Ibraheem, 2020).**

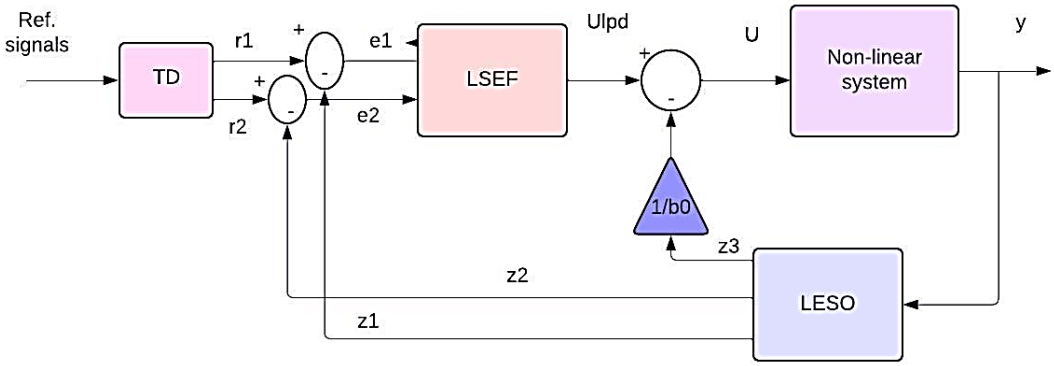

Figure 1. LADRC structure.

The proposed LADRC of **Fig. 1** is composed of three basic units, namely:

4.1 Tracking Differentiator (TD)

In **Fig. 1**, it is called the "signal profile generator" and is intended to handle transitions and replicate the derivative of the reference signal. The TD is suggested to be:

$$\dot{r_1} = r_2$$
$$\dot{r_2} = -r\ sign\ (r_1 - v(t) + \frac{r_2|r_2|}{2r} \quad (6)$$

Provides, up to the acceleration limit of r, the fastest tracking of v (t) and its derivative. This is why (6) is referred to as v (t)'s "tracking differentiator."

4.2 Linear State Error Feedback (LSEF)

In **Fig. 1**, it is also referred to as the linear controller. The LSEF reduces error and improves system performance when the LESO estimates the total disturbance, or $z3$. By omitting the integrator, a modified PID controller is used; this new controller is known as a linear proportional derivative (LPD) controller. The LESO will estimate all uncertainties, exogenous disturbances, and other discrepancies in the system and remove them from the nonlinear system by subtracting these estimated undesired signals from the input channel in a real-time behavior. This is where the idea to ignore the integrator portion comes from.

The outcome is a linearized system with a series of integrators leading to the relative value of a nonlinear system' relative degree (ρ), and the system already incorporates the integrator action. The recommended LPD controller is built as:

$$u(t) = k_p e(t) + k_d \frac{du}{dt} e(t) \quad (7)$$

From TD and LESO as:

$$e_1 = r_1 - z_1 \quad (8)$$
$$e_2 = r_2 - z_2 \quad (9)$$

Sub. Equ. (8) & (9) in Equ.(7) as:

$$U_{LPD} = k_p e_1 + k_d e_2$$
$$U_{LPD} = k_p(r_1 - z_1) + k_d(r_2 - z_2) \quad (10)$$

Once the whole disturbance has been subtracted from the input channel, the net control signal that activates the nonlinear system is as follows:

$$U = U_{LPD} - \frac{z_3}{b_0} \quad (11)$$

4.3 Linear Extended State Observer (LESO)

Its purpose is to measure and track uncertainties and disturbances. In **Fig. 1**, it is also referred to as the state and total disturbance observer. The design's proposed LESO equations are shown in (12):

$$\begin{cases} \dot{z_1} = z_2 + \beta_1 e \\ \dot{z_2} = z_3 + \beta_2 e + b_0 U \\ \dot{z_3} = \beta_3 e \end{cases} \quad (12)$$

Where $e = (y - z_1)$, $\beta_1 = 3w_0$, $\beta_2 = 3w_0^2$, $\beta_3 = w_0^3$, w_0 is the observer's bandwidth and should be optimized to give the minimum estimation error, z_1, z_2 are the estimated states of the nonlinear system, and z_3 is the estimated total disturbance, representing the unwanted dynamics, uncertainties, and exogenous disturbances. As illustrated in **Fig. 2**, the TWSBR system is a multi-loop system.

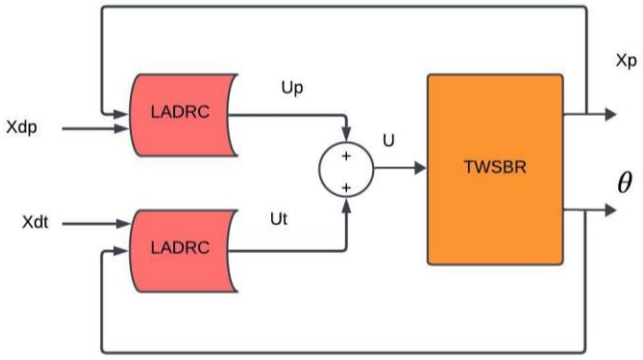

Figure 2. TWSBR system with LADRC configuration.

There is linear ADRC compensation in the position (x, y) controllers. We shall be focusing on the location (x) and angle (θ) systems in this study

5. SIMULATION AND RESULTS

MATLAB/Simulink is used to implement the TWSBR model with the LADRC, and the sampling time is set to ts = 0.01 seconds. As shown below, the LADRC unit's optimal parameter values are determined by using Genetic Algorithm (GA) optimization to the multi-objective OPI index minimization issue**(Allawi et al., 2019)**. The performance of the entire system was also assessed in this work using a practical multi-objective Performance Index (MOPI) shown this in **Fig.3**.

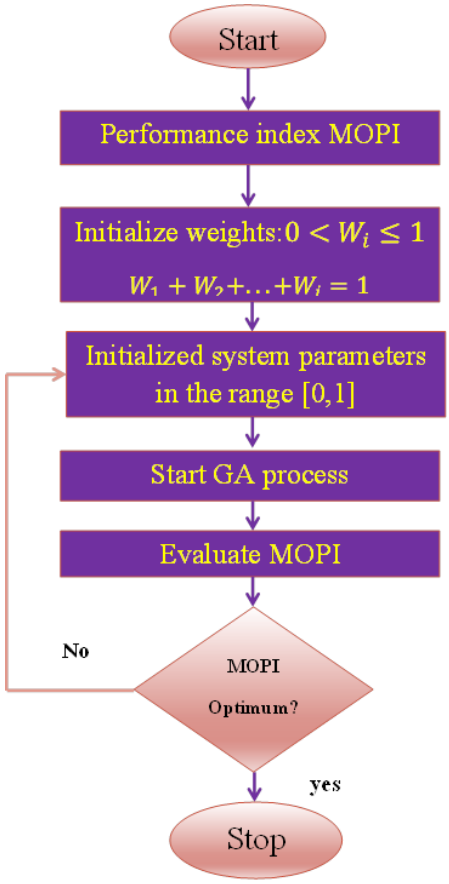

Figure 3. The flowchart of (GA).

It is expressed as follows and gauges how effective the suggested plan is:

$$OPI = w_1 * ISU + w_2 * ITAE + w_3 * ITSE \quad (13)$$

Where ISU , $ITAE$, and $ITSE$ represent the objective performance index for the system, respectively; w_1, w_2 *and* w_3 are weighting factors. To treat the system equally likely, where w_1, w_2 *and* w_3 are the weighting factors that satisfy $w_1 + w_2 + w_3$=1. According to that, they are set to w_1=0.4, w_2=0.2 and w_3=0.4. **Table 1** shows the description and mathematical representation of the performance indices.

Table 1. The performance's description and mathematical representation

PI	Description	Mathematical representation
ITAE	Integral time absolute error	$\int_0^{tf} t\|e(t)\|\,dt$
ITSE	The integral of the Square of the error	$\int_0^{tf} e^2(t)dt$
ISU	Integral of the Square of the control signal	$\int_0^{tf} u(t)^2\,dt$

Fig. 2 has a special drawing of a robot on two wheels that keeps itself balanced. This drawing shows the robot's design based on a smart control method.
In our quest to evaluate this robot's equilibrium maintenance, we undertook tests under certain distinct conditions presented in **Table 2** these represent the parameters of the robotic system. To simulate the system effectively, we employed an ode45 tool. The configuration for ADRC and PID controllers was determined as displayed in **Tables 3 to 6.**

Table 2. Parameters of TWSBR system

Parameter	Units
$\mathbf{M_p}$	3 kg
$\mathbf{M_w}$	0.5 kg
g	9.81 m/s^2
l	0.1 m
$\mathbf{r_w}$	0.1 m
$\mathbf{J_p}$	0.04 kg.m^2
$\mathbf{J_w}$	0.0025 $kg.m^2$
$\mathbf{k_m}$	0.0134 Nm/Amp
$\mathbf{k_e}$	0.1061 Vs/rad
R	1.9 Ω

Table 3. LESOs parameters

parameter	X_p Subsystem(0.8m)	θ Subsystem(0.8m)	X_p Subsystem(0.2m)	Θ Subsystem(0.2m)
w_0	3.211	0.0885	19.012	0.204
b_0	0.0756	0.09275	0.0756	0.09275

Table 4. TDs parameters

parameter	X_p ,θ Subsystem (at displacement 0.2 m)	X_p ,θ Subsystem (at displacement 0.8 m)
r_1	0.2335	0.2568
r_3	0.2611	0.2611

Table 5. LSEF parameters

parameter	X_p subsystem	Θ subsystem
k_1	0.01190	
k_2	75.2131	
k_3		125.95
k_4		6.2352

Table 6. PID parameters

parameter	X_p subsystem	Θ subsystem
K_p	43.2997	0.1340
K_d	30.3085	138.8370
K_i	75.7397	1.2232

It is evident from **Tables 7 and 8's** results that the optimization process involves making trade-offs between the performance indices. After switching the controller from PID to LADRC, which prioritizes reducing energy consumption, the Performance indices of the (x, θ) decreased. Utilizing LADRC to over 100% of the PID controller lowers the overall OPI at displacement (0.8m) and over 100% at displacement (0.2).

Table 7. Position and Angle Performance indices after applying step input using PID and LADRC controllers at the displacement command is 0.8(m).

Controller	ITAE	ITSE	ISU	OPI
PID	21.4360	5.0244	358600	1.4345e+05
LADRC	3.943525	0.069656	65.429655	26.9884

Table 8. Position and Angle Performance indices after applying step input using PID and LADRC controllers at the displacement command is 0.2(m).

controller	ITAE	ITSE	ISU	OPI
PID	4.8479	0.23034	8833	1765.26
LADRC	1.113891	0.008279	27.058385	4.8490

A comparison of the displacement reference's setting results between ADRC and PID controls:
Let's look at the outcomes achieved with Linear Active Disturbance Rejection Control (LADRC) - Proportional Derivative (PD) and compare them to standard PID controls by applying these different settings. The system starts in motion at the position. $x_p = 0.8$ meters, and $\theta_p = 0$, all under an interval of just 50 seconds. Look at **Figs. 4 and 5**; then start in motion at the position. $x_p = 0.2$ meters, and $\theta_p = 0$, at the same time, look at **Figs. 6 and 7** to see how the body tilts and moves during the TWSBR system test; Look at Table 9 to see state variables for state space for this system.

Table 9. State variables for the TWSBR system.

State variables	$\dot{x}$ at (0.8 m,0 rad)	$\dot{x}$ at (0.2 m,0 rad)
$\dot{x_1}$	8.734e-05	-0.0001727
$\dot{x_2}$	-0.01712	0.02571
$\dot{x_3}$	-4.217e-05	-6.23e-06
$\dot{x_4}$	0.002902	-0.004291

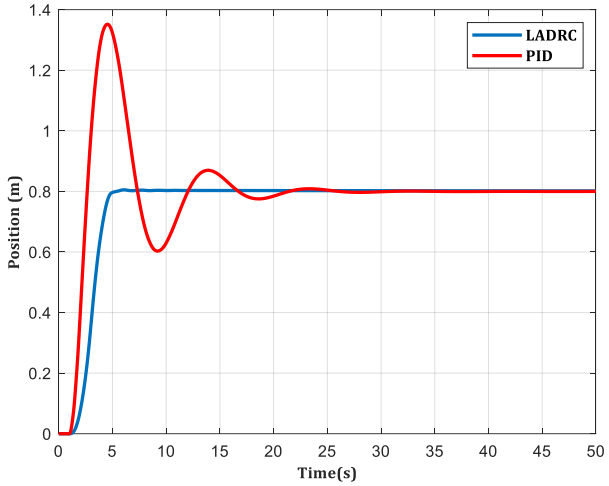

Figure 4. Output response of robot displacement at the shifting is 0.8(m).

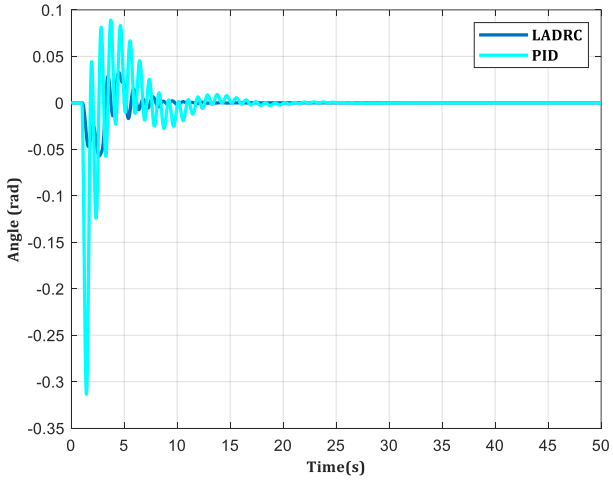

Figure 5. Output response of robot angle at the shifting is 0.8(m).

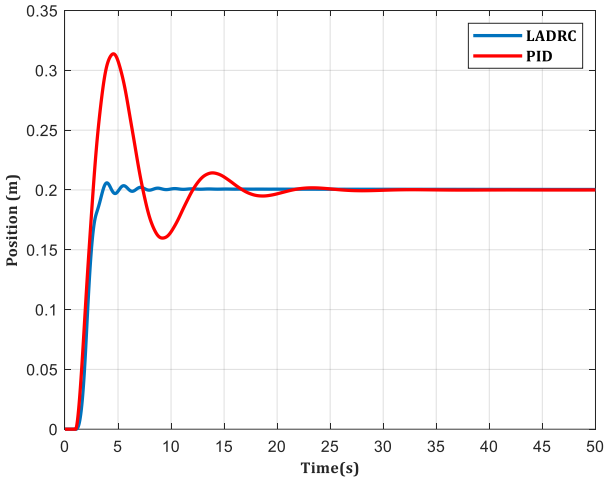

Figure 6. Output response of robot displacement at the shifting is 0.2(m).

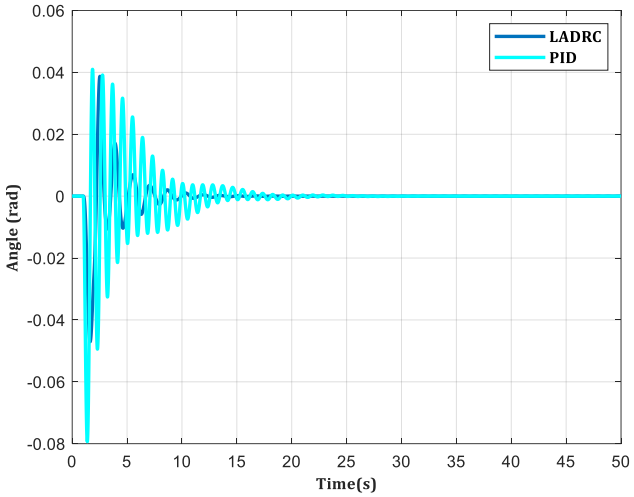

Figure 7. Output response of robot angle at the shifting is 0.2(m).

The results of **Figs. 5 and 7** demonstrate that the two LADRC controllers reduced the transition process time by over 200% in **Fig.4** and 4.2% in **Fig.7** when overshoot was 200% in **Fig.5** and 5.26% in **Fig.7** compared to the PID controller in the regulation of the robot body angle. Based on **Figs. 5 and 7**, we can observe that the two LADRC controllers reduced the transition process time by over 300% in **Fig.5** and over 200% in **Fig.7** the overshoot was around 75% in **Fig.4** and 53.11% in **Fig. 6** of the PID controller when controlling the robot shifting.

5.1. External Disturbance Case Study

The final test on the TWSBR system with a LADRC configuration aimed to guarantee consistent, accurate tracking despite external disruptions. This was determined by introducing an outside commotion in both (x_p, θ) at [1.6, 0.5] $N.m$ for timed periods of 20 seconds each **Figs. 8 to 11** show the correlating responses. Fascinatingly, different controllers had varied reactions! A notable example is how disruption led to considerable performance dips in Proportional Derivative (PD)-using LADRC controller—it registered drastic deviations over thirty percent from steady-state response levels during these interruptions.

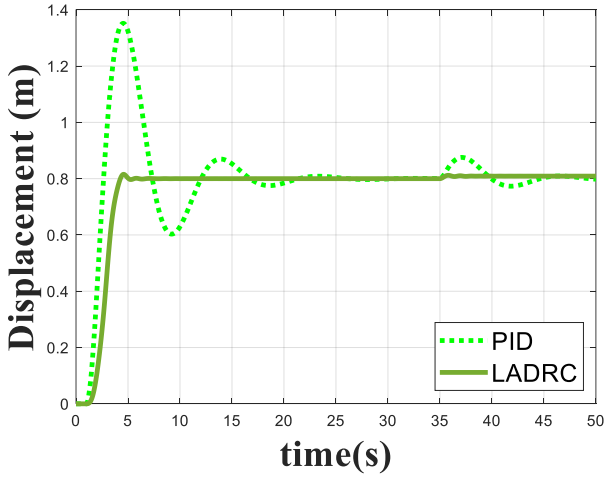

Figure 8. Output response of robot displacement with case study at the shifting is 0.8(m).

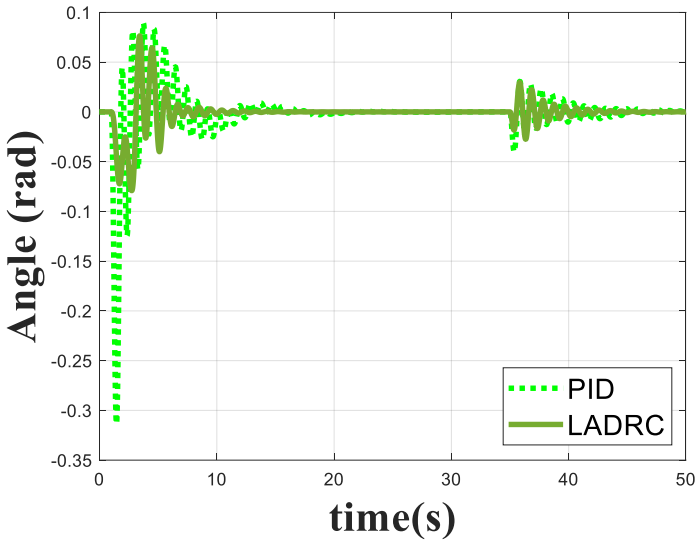

Figure 9. Output response of robot angle with case study at the shifting is 0.8(m).

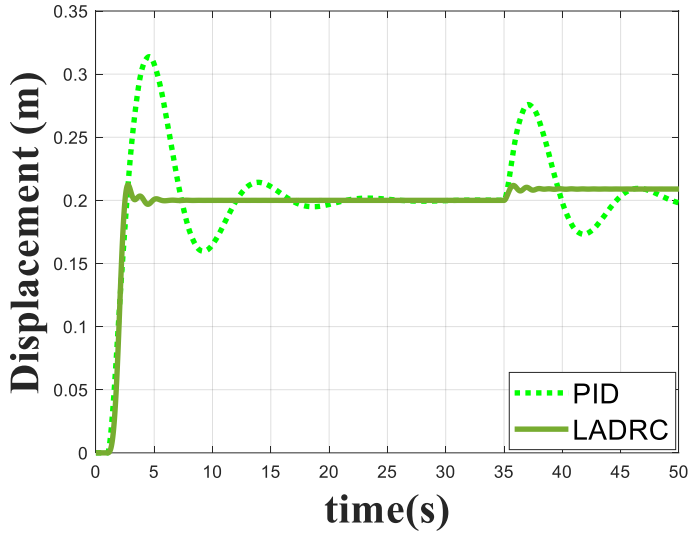

Figure 10. Output response of robot displacement with case study at the shifting is 0.2(m).

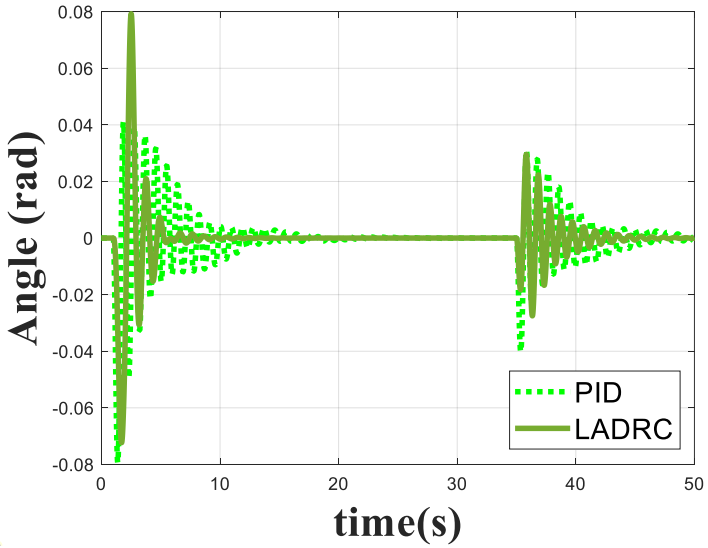

Figure 11. Output response of robot angle with case study at the shifting is 0.2(m).

6. CONCLUSIONS

In this paper, a two-wheeled robot that could balance itself. It's hard to control because it's complex; everything affects everything else, and we don't know all the details. This research used a special control method called ADRC. ADRC is good at handling systems with many variables without getting confused; it can adapt to changes well and keep things stable and separate, like the tilt and position of the robot. Tests have shown that ADRC works well at controlling things even when there are a lot of interfering factors, and the improvement over PID is over 90%, which is an excellent result for the TWSBR system.

NOMENCLATURE

Symbol	Description	Symbol	Description
b_0	A rough approximation of the coefficient b.	K_4	Derivative gain for PD controller of angle
g	Gravity, m/s^2	l	Length to the body's center of mass, m.
J_p	Inertia of the body, kg/m^2	M_p	Mass of body, kg.
J_w	Inertia of the wheel, kg/m^2	M_w	Mass of wheel, kg.
K_m	Motor torque constant, Nm/amp.	R	Nominal terminal resistance, Ω.
K_e	Back EMF constant, Vs/rad.	r_w	Radius of wheel, m.
K_p	proportional gain	r	The amplification coefficient
K_d	Derivative gain	r_1, r_2	TD tuning parameter for position
K_i	integral gain	r_3, r_4	TD tuning parameter for angle
K_1	proportional gain for PD controller of position	x_d	Desired constant
K_2	Derivative gain for PD controller of position	w_0	The observer's bandwidth
K_3	proportional gain for PD controller of angle	$\beta_{(1,2,3)}$	Observer gains

Credit Authorship Contribution Statement

Noor Abdul Ameer: writing the draft version. Ibraheem Kasim Ibraheem: Methodology, reviewing, and proofreading version.

Declaration of Competing Interest

The authors declare that they have no known competing financial interests or personal relationships that could have appeared to influence the work reported in this paper.

REFERENCES

Abbas, N.H. and Sami, A.R., 2018. Tuning of PID controllers for quadcopter system using cultural exchange imperialist competitive algorithm. *Journal of Engineering*, *24*(2), pp.80-99. https://doi.org/10.31026/j.eng.2018.02.06.

Abdul-Adheem, W.R., Ibraheem, I.K., Azar, A.T. and Humaidi, A.J., 2020. Improved active disturbance rejection-based decentralized control for MIMO nonlinear systems: comparison with the decoupled control scheme. *Applied Sciences*, *10*(7), p.2515. https://doi.org/10.3390/app10072515.

Al-Araji, A.S., 2014. Applying cognitive methodology in designing on-line auto-tuning robust PID controller for the real heating system. *Journal of Engineering*, *20*(09), pp.43-61. https://doi.org/10.31026/j.eng.2014.09.04.

Allawi, Z.T., Ibraheem, I.K. and Humaidi, A.J., 2019. Fine-tuning meta-heuristic algorithm for global optimization. Processes, 7(10), p.657. https://doi.org/10.3390/pr7100657.

Alonge, F., Cirrincione, M., D'Ippolito, F., Pucci, M., and Sferlazza, A., 2017. Active disturbance rejection control of linear induction motor. *IEEE Transactions on Industry Applications*, *53*(5), 4460-4471. https://doi.org/10.1109/ECCE.2016.7854817.

Ar-Ramahi, S.K.H., 2009. PID controller design for the satellite attitude control system. *Journal of Engineering*, 15(1), pp.3312-3320. https://doi.org/10.31026/j.eng.2009.01.06.

Curiel-Olivares, G., Linares-Flores, J., Guerrero-Castellanos, J.F. and Hernández-Méndez, A., 2021. Self-balancing based on active disturbance rejection controller for the two-in-wheeled electric vehicle, experimental results. *Mechatronics*, 76, p.102552. https://doi.org/10.1016/j.mechatronics.2021.102552.

Fu, C. and Tan, W., 2016. Tuning of linear ADRC with known plant information. *ISA transactions*, 65, pp.384-393. https://doi.org/10.1016/j.isatra.2016.06.016.

Gao, Z., 2003, June. Scaling and bandwidth-parameterization based controller tuning. In *Acc.*(4), pp. 989-994. https://doi.org/10.1109/ACC.2003.1242516.

Han, J., 2002. From PID technology to auto disturbance rejection control technology. *Control Engineering of China*, 9(3), pp.13-18. https://doi.org/10.1109/TIE.2008.2011621.

Han, J., 2009. From PID to active disturbance rejection control. *IEEE transactions on Industrial Electronics*, 56(3), pp.900-906. https://doi.org/10.1109/TIE.2008.2011621.

Han, J.Q., 1995. Nonlinear state error feedback control law-NLSEF. In *Chinese Univ Pr* (p. 211).ISBN: 9622017010, 9789622017016.

Hernández-Méndez, A., Linares-Flores, J., Sira-Ramírez, H., Guerrero-Castellanos, J.F. and Mino-Aguilar, G., 2017. A backstepping approach to decentralized active disturbance rejection control of interacting boost converters. *IEEE Transactions on Industry Applications*, 53(4), pp.4063-4072. https://doi.org/10.1109/TIA.2017.2683441.

Huang, Y. and Xue, W., 2014. Active disturbance rejection control: Methodology and theoretical analysis. *ISA transactions*, *53*(4), pp.963-976. https://doi.org/10.1016/j.isatra.2014.03.003.

Ibraheem, I. K., 2020. Anti-disturbance compensator design for unmanned aerial vehicle. *Journal of Engineering*, *26*(1), pp. 86-103. https://doi.org/10.31026/j.eng.2020.01.08.

Ibraheem, I.K. and Ibraheem, G.A., 2016. Motion control of an autonomous mobile robot using modified particle swarm optimization based fractional order PID controller. *Engineeing Technology Journal*, *34*(13), pp.2406-2419. https://doi.org/10.30684/etj.34.13A.4.

Kang, C., Wang, S., Ren, W., Lu, Y., and Wang, B., 2019. Optimization design and application of active disturbance rejection controller based on intelligent algorithm. *IEEE Access*, *7*, 59862-59870. https://doi.org/10.1109/ACCESS.2019.2909087.

Jin, H., Song, J., Lan, W. and Gao, Z., 2020. On the characteristics of ADRC: A PID interpretation. Science China. Information Sciences, 63(10), p.209201. https://doi.org/10.1007/s11432-018-9647-6.

Lei, Y., Xu, J., Ni, Y., Wang, Z. and Liu, W., 2019, May. Application of ADRC in track alignment detection system. *In 2019 IEEE 8th Data Driven Control and Learning Systems Conference (DDCLS)* (pp. 939-945). IEEE. https://doi.org/10.1109/DDCLS.2019.8909066.

Li, Y., Wang, J., and Zhang, Y.J., 2015. Self-tuning method for a linear active disturbance rejection controller. *Chinese Journal of Engineering*, 37(11), pp.1520-1527. https://doi.org/10.13374/j.issn2095-9389.2015.11.019.

Lima-Pérez, A., Díaz-Téllez, J., Gutiérrez-Vicente, V., Estévez-Carreón, J., Pérez-Pérez, J., García-Ramirez, R.S. and Chávez-Galán, J., 2021, November. Robust control of a two-wheeled self-balancing mobile robot. In *2021 International Conference on Mechatronics, Electronics and Automotive Engineering (ICMEAE)* (pp. 196-201). IEEE. https://doi.org/10.1109/ICMEAE55138.2021.00038.

Linares-Flores, J., García-Rodríguez, C., Sira-Ramirez, H. and Ramírez-Cárdenas, O.D., 2015. Robust backstepping tracking controller for low-speed PMSM positioning system: Design, analysis, and implementation. *IEEE Transactions on industrial informatics*, 11(5), pp.1130-1141.. https://doi.org/10.1109/TII.2015.2471814.

Linares-Flores, J., Barahona-Avalos, J.L., Sira-Ramirez, H. and Contreras-Ordaz, M.A., 2012. Robust passivity-based control of a buck–boost-converter/DC-motor system: An active disturbance rejection approach. *IEEE Transactions on Industry Applications*, 48(6), pp.2362-2371. https://doi.org/10.1109/TIA.2012.2227098.

Liu, Z.H., Zhang, Y.J., Zhang, J. and Wu, J.H., 2011. Active disturbance rejection control of a chaotic system based on immune binary-state particle swarm optimization algorithm. *Acta Phys. Sin.* https://doi.org/10.7498/aps.60.019501.

Liu, W., Zhang, B., Guo, S., Shi, J., Ji, M. and Zheng, S., 2023. Research on active disturbance rejection control technology of two-wheel self-balancing robot. *In 2023 5th International Conference on Electrical Engineering and Control Technologies (CEECT)*. (pp. 325-332). IEEE. https://doi.org/10.1109/CEECT59667.2023.10420693.

Mohammed, I.A., Mahir, R.A. and Ibraheem, I.K., 2011. Robust controller design for load frequency control in power systems using state-space approach. *Journal of Engineering*, *17*(02), pp.265-278. https://doi.org/10.31026/j.eng.2011.02.06.

Mtolo, S. N., and Saha, A. K., 2021. A review of the optimization and control strategies for fuel cell power plants in a microgrid environment. *IEEE Access*, *9*, 146900-146920. https://doi.org/10.1109/ACCESS.2021.3123181.

Paulescu, F.C., Szeidert, I., Filip, I. and Vasar, C., 2021, May. Two-wheeled self-balancing robot. *In 2021 IEEE 15th International Symposium on Applied Computational Intelligence and Informatics (SACI),* pp. 33-38. IEEE. https://doi.org/10.1109/SACI51354.2021.9465568.

Qi, X.H., Li, J. and Han, S.T., 2013. Adaptive active disturbance rejection control and its simulation based on BP neural network. *Acta Armamentarii*, 34(6), p.776. https://doi.org/10.3969/j.issn.1000-1093.2013.06.019.

Sira-Ramírez, H., Luviano-Juárez, A., Ramírez-Neria, M., and Zurita-Bustamante, E. W. 2017. *Active disturbance rejection control of dynamic systems: A flatness based approach*. Butterworth-Heinemann. ISBN: 978-0-12849868-2

Sira-Ramírez, H., Linares-Flores, J., García-Rodríguez, C. and Contreras-Ordaz, M.A., 2014. On the control of the permanent magnet synchronous motor: An active disturbance rejection control approach. *IEEE Transactions on Control Systems Technology*, 22(5), pp.2056-2063. https://doi.org/10.1109/TCST.2014.2298238.

Sira-Ramírez, H., Hernández-Méndez, A., Linares-Flores, J. and Luviano-Juárez, A., 2016. Robust flat filtering DSP based control of the boost converter. *Control Theory and Technology*, 14(3), pp.224-236. https://doi.org/10.1007/s11768-016-6025-6.

Tan, W. and Fu, C., 2015. Linear active disturbance-rejection control: Analysis and tuning via IMC. *IEEE Transactions on Industrial Electronics*, 63(4), pp.2350-2359. https://doi.org/10.1109/TIE.2015.2505668.

Wang, Z., Zu, R., Duan, D., and Li, J., 2019. Tuning of ADRC for QTR in transition process based on NBPO hybrid algorithm. *IEEE Access*, *7*, 177219-177240. https://doi.org/10.1109/ACCESS.2019.2957318.

Wei, Z., and Huang, R., 2022. Active disturbance rejection control of two-wheeled self-balancing vehicle. In *2022 China Automation Congress (CAC)* (pp. 4086-4091). IEEE. https://doi.org/10.3390/asi7020022.

Xue, W., Bai, W., Yang, S., Song, K., Huang, Y. and Xie, H., 2015. ADRC with adaptive extended state observer and its application to air–fuel ratio control in gasoline engines. *IEEE Transactions on Industrial Electronics*, 62(9), pp.5847-5857. https://doi.org/10.1109/TIE.2015.2435004.

Ye, D. P., Yu, J. M., and Zhou, Y. Z., 2013. Control simulation for two-wheeled self-balancing robot linear move based on active disturbance rejection controller. *Advanced Materials Research*, *644*, 129-133. https://doi.org/10.4028/www.scientific.net/AMR.644.129.

Zheng, Q. and Gao, Z., 2016. Active disturbance rejection control: Between the formulation in time and the understanding in frequency. *Control Theory and Technology*, *14*, pp.250-259. https:/doi.org/10.1007/s11768-016-6059-9.

التحكم الخطي في رفض الاضطراب النشط (ADRC) للروبوت ذاتي التوازن ثنائي العجلات

نور عبدالامير مطلك*، ابراهيم قاسم ابراهيم

قسم الهندسة الكهربائية، كلية الهندسة، جامعة بغداد، بغداد، العراق

الخلاصة

يعتمد تطبيق روبوت التوازن الذاتي ذو العجلتين على مهام العالم الحقيقي بشكل حاسم على قدرته على رفض الاضطرابات بشكل فعال. الهدف هو تصميم وحدتي تحكم نشطتين لرفض الإزعاج (ADRCs) لزاوية الجسم والإزاحة، على التوالي، لنظام روبوت ذاتي التوازن ذو عجلتين، والذي يصعب التحكم فيه بسبب الاقتران القوي، وعدم الخطية، وعدم اليقين في المعلمات. استنادًا إلى ديناميكيات النظام، تم تصميم إطار التحكم ADRC لتقدير وتعويض أخطاء النمذجة والاضطرابات عبر الإنترنت. تُستخدم عمليات المحاكاة الرقمية لإثبات فعالية ADRC في مجموعات وحدات التحكم المختلفة، باستخدام Simulink MATLAB 2022a وضبط المعلمات بواسطة الخوارزمية الجينية (GA) لضمان أداء عابر جيد والمساعدة في عملية اختيار معلمات التصميم. تُظهر الدراسات التي أجريت على مركبة حقيقية ذاتية التوازن ذات عجلتين أن نظام ADRC الذي تم إنشاؤه يسمح للمركبة بالعمل بشكل أكثر اتساقًا وفعالية عند مقارنتها بوحدة التحكم PID (التناسبية – المتكاملة – المشتقة) تحت نفس إعداد المعلمة.

الكلمات المفتاحية: روبوت التوازن الذاتي بعجلتين (TWSBR)، التحكم النشط في رفض الإزعاج (ADRC)، التحكم في المشتق النسبي التكاملي (PID)، الخوارزمية الجينية (GA).